

# **Risk Assessment of Outdoor Micron Particulate Matters Inhaled in the Respiratory System of a Standing Mannequin in a Room Ventilated by a Wind Catcher**

**Farhad Zare\***

*School of Mechanical Engineering, Shiraz University, Shiraz, Iran*

**\*Corresponding author:** Farhad Zare, School of Mechanical Engineering, Shiraz University, Shiraz, Iran

**Received:** January 28, 2024

**Published:** March 03, 2025

## **Abstract**

**Background and Objective:** In this study the potential of inhaled micro particles in the respiratory system of a mannequin standing in the middle of a room ventilated by a wind catcher was assessed.

**Methods:** The realistic model of a nasal route up to the nasopharynx was obtained from Computed tomography (CT) scan images, and then attached to the nostrils of a standing mannequin. The mannequin was positioned in the middle of a room ventilated by an optimum wind catcher. Micro particles ranging from 1  $\mu\text{m}$  to 10  $\mu\text{m}$  were released from the wind catcher opening with the same velocity as the air fluid flow through a UDF and the inhaled particles were evaluated.

**Results:** The results show that the maximum and minimum inhaled particle percentage belong to the particles with 1- $\mu\text{m}$  and 5- $\mu\text{m}$  diameters with the value of 0.0164 and 0.0136, respectively. Also, the aspiration fraction for these particles is 82 and 68 percent. The minimum and maximum percentage of inhaled particles passing the nasopharynx and going out of the nasal route are 88.35 and 71.50 percent that are associated with 1- $\mu\text{m}$  and 10- $\mu\text{m}$  particles.

**Conclusion:** Based on the obtained results and according to the number of particles delivered to the outlet of the nasal cavity, the most detrimental particles to the respiratory system in the order are: 1, 2, 2.5, 3, 4, 7, 9, 6, 8, 5, and 10. This order according to the mass of particles delivered is: 10, 9, 8, 7, 6, 5, 4, 3, 2.5, 2, and 1. The results of this study provide the required data for specialists to evaluate inhalation toxicology and implement necessary measures regarding wind catchers.

**Keywords:** Risk assessment; Particulate matter; Respiratory system; Nasal cavity; Wind catcher

## **Introduction**

Now that the shortage of conventional sources of energy is more sensible than ever, using sustainable sources is dramatically considering. As anything else, these sources have their own advantages and drawbacks. A wind catcher is one of those devices that can be used to harness the power of the wind to circulate air in a room. It can enhance the natural ventilation rate due to increasing air movement. Along with using a wind catcher to create natural ventilation and consequently, to save energy consumption, it may produce some breathing problems as a result of particulate matters coming indoor.

In terms of natural ventilation, the work done by [1] assessed 12 different scenarios with different atrium ceiling shapes to evaluate the effects of the atrium ceiling on catching sea breeze, indoor thermal comfort, and natural ventilation in the coastal buildings. Finally, they found that Specimen 12 pro-

vided the highest volumetric flow rate and the best condition in terms of natural ventilation. [2] Investigated the Association between outdoor air pollution and chronic rhinosinusitis. They revealed that exposure to outdoor air pollutants such as ozone ( $\text{O}_3$ ), black carbon BC, nitrogen dioxide ( $\text{NO}_2$ ), and particulate matters are responsible for increased symptom severity in patients who suffer from chronic rhinosinusitis (CRS). Also, it can be inferred that these matters might cause problems for normal people in the real-life situation. [18] Investigated the transportation and deposition of pollutant particulate matters in micro- and nano-scales in the mouth-throat and tracheobronchial lung airways of a human lung using computational fluid dynamics (CFD). They reported that the deposition efficiency of 10- $\mu\text{m}$  particles varied between 99.8% to 64.28%, while this value for 5- $\mu\text{m}$  nanoparticles was only 10%. It means that the majority of nanoparticles can pass through the lung and even enter the blood circulation system and cause serious problems.

Although the nasal route gives an opportunity for delivering drug particles as the works of [3-5], hazardous particulate matters can enter the human respiratory system as investigated by [6-10], assessed the deposition of micron-sized particles in a realistic human nasal cavity. Their results showed that micron particle exposure was dependent on a couple of factors such as: anatomical shape, airflow dynamics, and particle inertia. Besides, the majority of particles were deposited in the main passage of the nasal cavity.

Using a wind catcher can be a double-edged sword. Actually, it can be used for ventilating a room and reducing indoor particulate matters or it can bring them to the room as a result of the natural ventilation purpose. Even though the privilege of using wind catchers is acknowledged, particulate matters entering the space can be detrimental to the human respiratory system.

**Methods**

**Model reconstruction**

After CFD simulations of 23 cases with various size and position of the outlet openings [11], showed that the configuration of a one-sided wind catcher with a window in the middle of the leeward facade has advantages over the other configurations in terms of induced airflow rate and air change efficiency. Consequently, to reach the main purpose of this study, a mannequin is positioned in their proposed configuration. The nasal geometry used in this study is the same as that of applied by [3]. Actually, this model replicates the realistic nasal airway with all paranasal sinuses belonging to an Asian female of 42 years of age. The only difference is the segmented parts. Materialise 3-matic 11.0 was used to segment the most important parts; Some of them were splitted by planes and the others by curves due to the meandrous path, the complexity and high curvature of the geometry. For the validation purpose of the nasal cavity, a simple model including just the main airway was used as demonstrated in **Figure 1**.

As it can be seen in **Figure 2** the respiratory system includes the main airway and all paranasal sinuses up to the end of the nasopharynx were attached to the mannequin depicted in **Figure 3**. The reason for this selection and not going deeper is that the nasal cavity has two 90-degrees bends for filtering external particulate matters and if any particles passing through them without deposition, they are considered as risk to the respiratory system and some modifications must be done in terms of the wind catcher. In other words, any particles escaping from the nasopharynx are detrimental to the lungs regardless of their further deposition pattern.

The final computational domain is depicted in **Figure 4** that demonstrates the mannequin standing in the middle of the room and facing the wind catcher.

**Grid generation**

Due to the complexity of the geometry, the unstructured mesh type was used for capturing the flow over the mannequin and in the nasal cavity with triangular surface meshes and tetrahedral volume meshes with prism layers.

It's been tried to refine the mesh as much as possible. But there are two limitations: The first is the y-plus range for the Enhanced Wall modeling method for turbulence modeling near the walls and the other is forced based on the Lagrangian approach of particle tracking. Actually, the first layers must be

small enough to capture the viscous sub-layer; Also, the DPM module in Ansys Fluent is a point particle model and so height of the first mesh elements have to be larger than the diameter of particles. In general, it means that each particle must not occupy more than one cell.

Different mesh cut planes of the mesh are demonstrated in **Figure 5**.

**Airflow modeling**

Montazeri, et al., [3] showed that the realizable k-ε turbulence model will balance accuracy against computational expenses in comparison with Large-Eddy Simulation (LES), the standard k-ε, and the RNG k-ε model for cross-ventilation using wind catchers. So, this model is implemented in this study for simulating the air flow field.

**Discrete phase modeling**

Peeters et al., [2] stated that particles in the (PM<sub>2.5</sub>) and (PM<sub>10</sub>) size ranges are dangerous for human health and also [12] had a statistical study and reported that in the rooms of roadside houses with natural ventilation outdoor air is a significant source of (PM<sub>2.5</sub>). Furthermore, [13] reported that particles with diameter less than 10 μm have the most effect on human health. So, in this study particulate matters (PM) in micron range will be investigated (1-10 μm).

In the present study, the lagrangian approach is used to pursue individual particles until they reach their fate. In this manner the inertia of a particle is equal to the summation of all forces acting on the particle and so the differential equation of motion for each particle is given in Eq. 1. It's clearly evident that the drag and gravitational forces are considered and all other seven natural forces such as virtual mass force, pressure gradient force, forces in moving reference frames, thermophoretic force, brownian force, saffman's lift force, magnus lift force, and buoyancy effect in the air are neglected.

$$\frac{du_p}{dt} = F_D(u - u_p) + g \tag{1}$$

Where

$$F_D = \frac{18\mu}{\rho_p d_p^2} \frac{C_D Re_p}{24} \tag{2}$$

$$C_D = a_1 + \frac{a_2}{Re_p} + \frac{a_3}{Re_p^2} \tag{3}$$

$$Re_p = \frac{\rho d_p |u_p - u|}{\mu} \tag{4}$$

**Boundary and initial conditions**

It will be more realistic to use atmospheric boundary layer (ABL) profiles for velocity, turbulent kinetic energy, and turbulence dissipation rate at the inlet boundary as implemented in the present study [14]:

$$u(z) = \frac{u_{ABL}^*}{\kappa} \ln\left(\frac{z + z_0}{z_0}\right) \tag{5}$$

$$k(z) = 3.3u_{ABL}^{*2} \tag{6}$$

$$\epsilon(z) = \frac{u^{*3}}{\kappa(z + z_0)} \tag{7}$$

Where Z<sub>0</sub> is the aerodynamic roughness length, which is 0.03 m for the flat terrain with grass surrounding the building. It is also used to calculate the roughness height (ks) with the value of 0.5 for the roughness constant Cs by the equation of [15]:

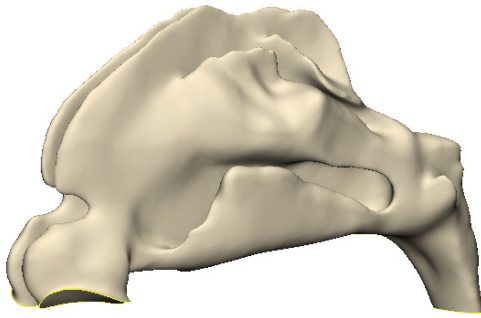


Figure 1: Just nasal cavity geometry for validation purpose.

$$k_s = \frac{9.793z_0}{C_s} \tag{8}$$

All other walls have zero roughness height ( $k_s = 0$ ). Symmetry type conditions are specified at the side surfaces as well as at the top surface of the computational domain. For the outlet plane of the domain, zero-gauge static pressure is implemented, while for the outlet surface of the nasal cavity a negative pressure is applied to duplicate the realistic condition of breathing.

**Results**

One of the roles of the human nasal cavity is to filter unwanted aerosols. As stated before, for the convenience of computational expenses the entire respiratory system is not modeled and includes the nasal airway up to the nasopharynx; So, if particles go further, they will be considered as risk to the lungs. Besides, the deposition of particles on some surfaces could be harmful. One of these surfaces could be the olfactory region that is connected to blood vessels.

**Computational model validation**

In this study validation of the computational model consists of two separate parts: The nasal geometry and the air flow field due to natural ventilation; And then these two regions will be merged by means of the mannequin standing in the middle of the room.

**Validation of the nasal geometry**

For validating the nasal airway geometry, a model without any sinuses was reconstructed as the benchmark models in the literature [16,17] and illustrated in **Figure 1**. [17] Investigated the effect of surface roughness on the impaction parameter. These researchers constructed three models with different roughness and labeled them as a, b and c. The case with the smoothest surface belongs to [17] (model c) and they showed that this model will give the most accurate results in terms of particle deposition. In addition, they showed that the model used by [16] is too rough to give reliable results. As illustrated in Figure 6, the model used by [16] is highly rough and overestimates the deposition efficiency in comparison with the three others. Additionally, by referring to this figure it can be seen that by approaching the volumetric flow rate of their study, the results of the present study get better. The only slight differences can be attributed to the difference in the shape of two geometries.

**Validation of the air flow field**

For validating the boundary conditions, especially the atmospheric boundary layer profile a simple model of the wind catcher without the nasal cavity, sinuses, and the mannequin was selected. After doing the grid study and comparing with the results obtained by [11], according to **Figure 7a** and **Figure**

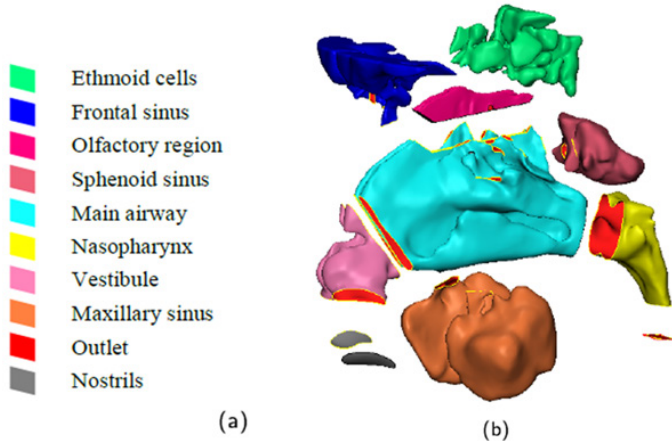


Figure 2: Disassembled parts: (a) Names; (b) parts.



Figure 3: The mannequin.

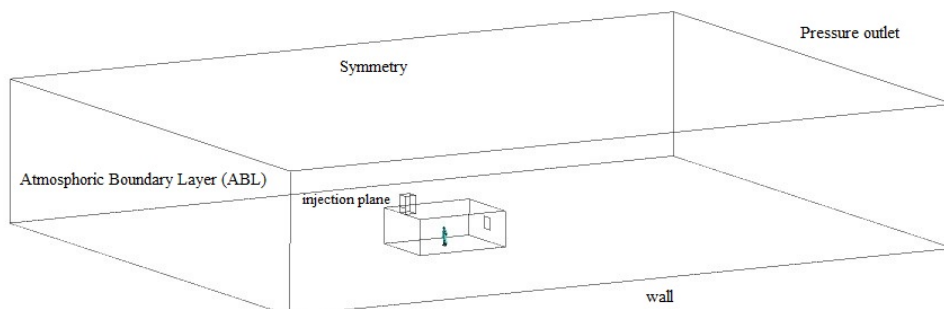


Figure 4: Computational domain.



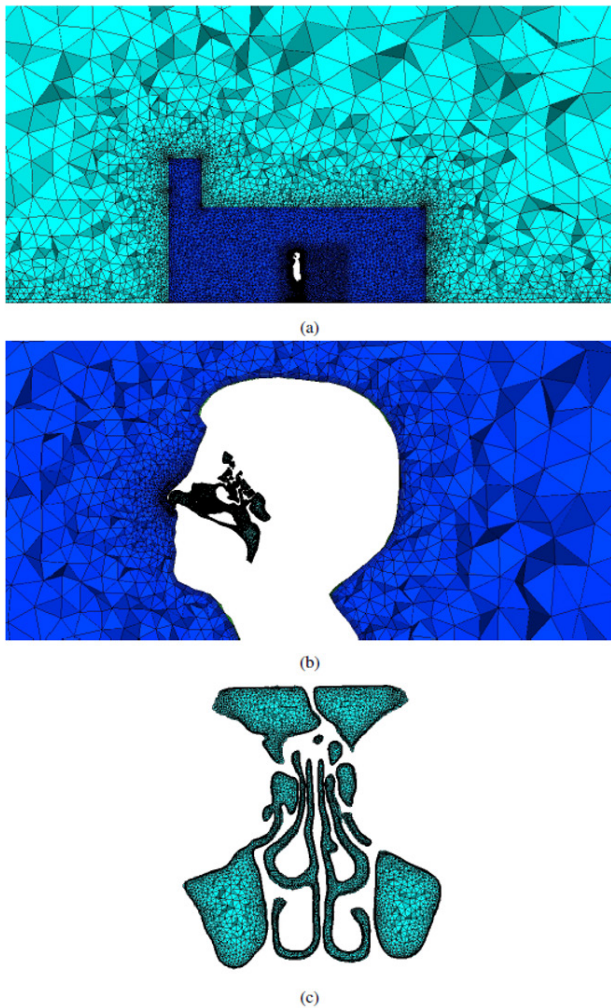


Figure 5: Mesh cut plane at: (a) Middle of the computational domain; (b) Lateral plane; (c) Coronal plane.

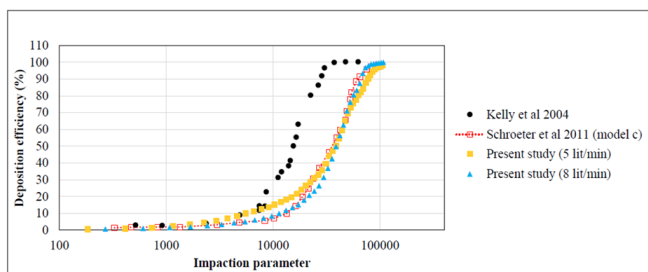


Figure 6: Impaction parameter.

7b the grid resolution with 2 million cells was selected which shows good agreement with the benchmark data.

**Fluid flow for the main case**

After doing the validations, the nasal route was connected to the mannequin and the mannequin was positioned in the middle of the room. For solving the governing equations and more accuracy, the Enhanced Wall Treatment modeling method except for the rough wall of the ground is used. In this manner, the first cells must be placed in the viscous sub-layer and the process of particle tracking will be more accurate, although it's computationally expensive for such a large domain. In addition, there is another obligation for the height of the first cells; Actually, it must be larger than the diameter of the particles; Because, Ansys Fluent uses point particle model; Therefore, the initial height for cells is 100 micron that is greater than the largest particles of 10 micron. In the context of grid study, three different grids were tested according to Table 1. This procedure culminated in the decision of the mesh with 3/577/989

elements. The reason for this selection is that changing in the magnitude of velocity and pressure is negligible for different lines for the second and third mesh sets as showed for velocity magnitude in Figure 8 and for pressure value in Figure 9.

For the main case, the velocity contour across a plane in the middle of the room is illustrated in Figure 10 and the streamlines are depicted in Figure 11. The streamlines are helical and almost symmetrical after entering the room through the wind catcher and the slight difference can be attributed to the asymmetrical shape of the mannequin. This helical path will increase the potential risk of the particles; Because they will cover more space in this situation in comparison with straight pathlines.

**Particle deposition for the main case**

In this part of the present study, the final results will be demonstrated and discussed. For reducing the computational cost, the injection of particles was done in two different stages. At the first stage they were injected at the wind catcher opening with the velocity of the air flow field by using a UDF (User Defined Function). After testing 10/000, 1/000/000, and 4/000/000 particles and the maximum number of iterations of 50/000, 100/000, 200/000, and 400/000, 1/000/000 particles with 200/000 maximum number of iterations were selected; And at the second stage, the particles were injected from the nostrils with the injected velocity equals to the flow velocity. Again 500/000, 1/000/000, 2/000/000, and 3/500/000 particles with 50/000 and 100/000 maximum number of iterations. The results of the regional particle deposition showed that 2/000/000 particles with 50/000 gave acceptable accuracy. One of the most important factors for evaluation of the risk of inhaled particles is Aspiration Fraction (AF). It is shown in Figure 12 and defined as:

$$AF\% = \frac{N_{inhaled}}{N_{total}} \times \frac{\text{air flow rate at the injection plane}}{\text{inhalation flow rate}} \tag{9}$$

Another useful factor is the particle number percentage inhaled through the nasal cavity. It can be obtained by dividing the number of inhaled particles through the nostrils by the total injected particles and is illustrated in Figure 13.

$$\text{inhaled particle percentage} = \frac{N_{inhaled}}{N_{injected}} \times 100 \tag{10}$$

For the nasal cavity the deposition fraction (%) will be the best option. It is showed in Figure 14 and defined as:

$$\text{Deposition Fraction} = \frac{N_{deposited}}{N_{injected}} \times 100 \tag{11}$$

To be more accurate the exact value of the deposition fraction is brought in Table 2. The deposited particles inside the room space is depicted in Figure 15. The majority of 1-μm particles are deposited on the ceiling, because their trajectories are like the streamlines and the gravitational force has almost no effects on them. On the other hand, the particles with 10-μm diameters are heavy enough to be deposited on the ground and they show almost no deposition on the ceiling.

**Discussion**

In terms of inhaled particle percentage, the maximum value belongs to the particles with 1- and 2-micron diameters as illustrated in Figure 13. 2-μm particles have more deposition on the roof. But, the less deposition of these particles on the wind catcher and ceiling walls due to the more gravitational force

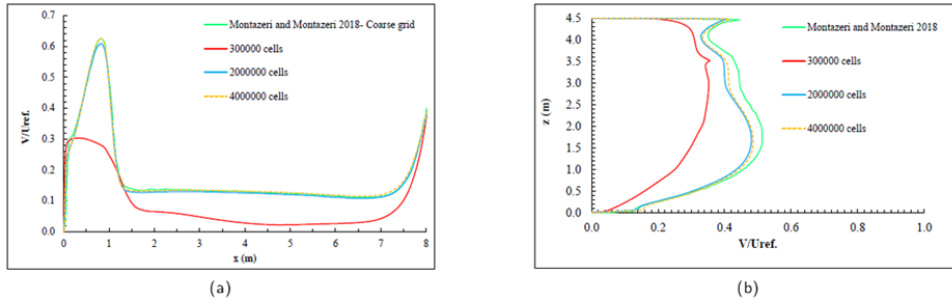


Figure 7: Results for the grid study and flow field validation (a) Along the horizontal line (b) Along the vertical line.

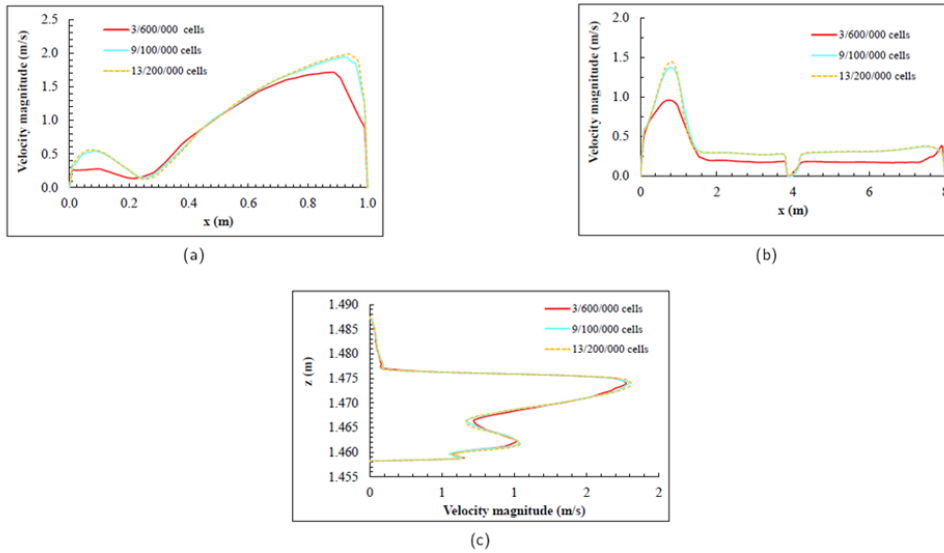


Figure 8: Grid study based on velocity magnitude for lines: (a) wind catcher inside diagonal; (b) across the mannequin; (c) the right vestibule.

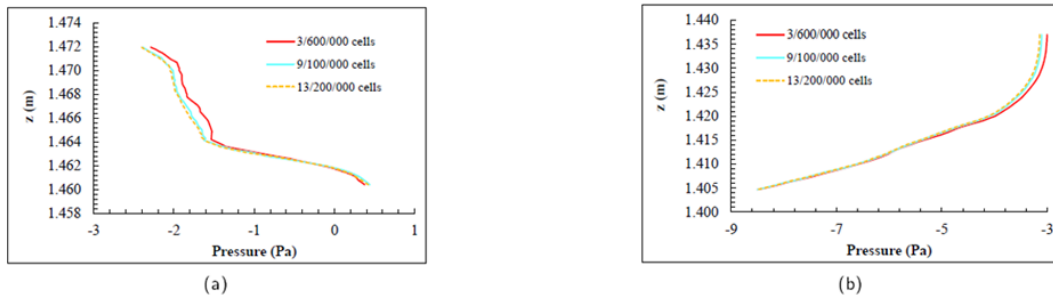


Figure 9: Grid study based on pressure value for lines: (a) the left nostril; (b) the nasopharynx.

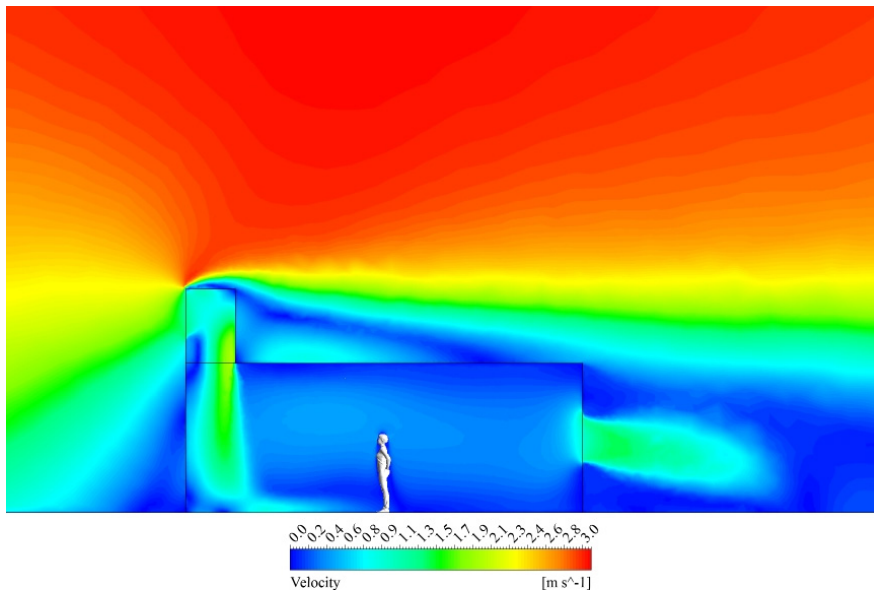


Figure 10: velocity contour on the middle plane.

Table 1: Number of mesh elements for grid study.

Surrounding	Room	Nasal cavity	Total
956452	1134401	1487136	3577989
4625314	2289524	2190888	9105726
6723231	3393540	3085809	13202580

Table 2: The values of deposition fraction for the nasal route.

Region	1 $\mu\text{m}$	2 $\mu\text{m}$	2.5 $\mu\text{m}$	3 $\mu\text{m}$	4 $\mu\text{m}$	5 $\mu\text{m}$	6 $\mu\text{m}$	7 $\mu\text{m}$	8 $\mu\text{m}$	9 $\mu\text{m}$	10 $\mu\text{m}$
Ethmoid cells	0.1144	0.1332	0.1509	0.1732	0.2282	0.3094	0.4205	0.5016	0.5692	0.6827	0.7207
Frontal sinus	0.0044	0.004	0.0047	0.0063	0.0091	0.0161	0.0217	0.0321	0.039	0.0571	0.0636
Olfactory region	0.0298	0.0296	0.0298	0.0249	0.018	0.0164	0.0149	0.0152	0.0097	0.0129	0.0058
Sphenoid sinus	0.0024	0.0029	0.0012	0.0009	0.0017	0.0005	0.0001	0	0	0	0
Main airway	3.352	3.5843	3.7456	3.8423	4.308	4.9008	5.7041	6.5106	8.1283	9.8689	11.5735
Nasopharynx	1.3803	1.4218	1.4302	1.4549	1.515	1.5683	1.6541	1.8906	2.3574	2.7347	3.0529
Vestibule	6.3691	6.535	6.6506	6.8126	7.2438	7.8211	8.597	9.5446	10.7839	11.915	12.8555
Maxillary sinus	0.0038	0.015	0.0198	0.0236	0.0375	0.0542	0.0757	0.091	0.0986	0.0949	0.0945
Outlet	88.3494	87.9952	87.7992	87.5058	86.5145	85.1774	83.3728	81.2568	77.8849	74.4929	71.5012

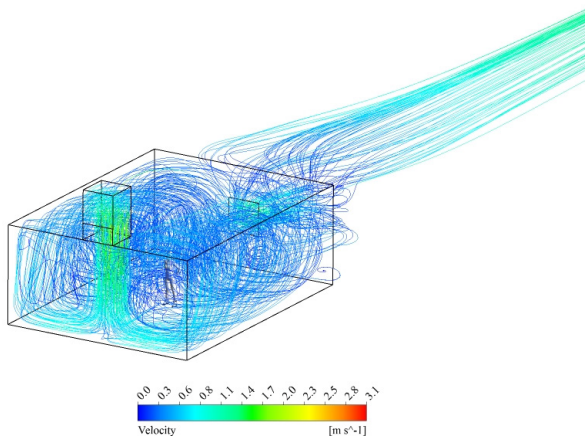


Figure 11: Streamlines entering the room.

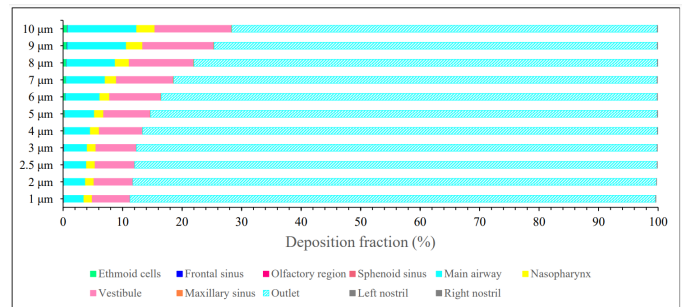


Figure 14: Deposition fraction for the nasal route.

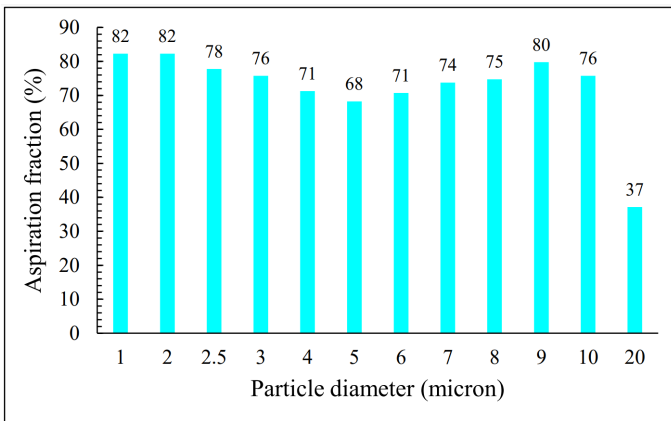


Figure 12: Aspiration fraction.

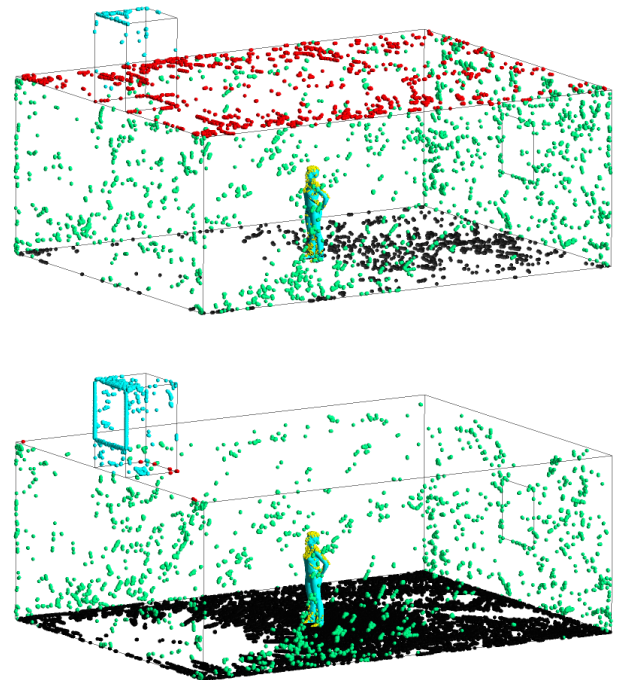


Figure 15: Deposited particles: (a) 1 micron; (b) 10 micron.

has counterbalance the effect of the first factor and has given them more chance to be inhaled. After 2 micron the gravitational force has become more and the deposition fraction on the ceiling has decreased and, on the ground, has increased. So, the particles that had not been deposited on the ceiling have been too high to be inhaled. consequently, the inhaled percentage has continued decreasing until 5 microns. After this diameter, the particles have been pulled down to the breathing zone and so the percentage has been increased. Again, after the diameter of 9 micron, the particles had been too low and near the building ground to be inhaled and so the inhalation of particles

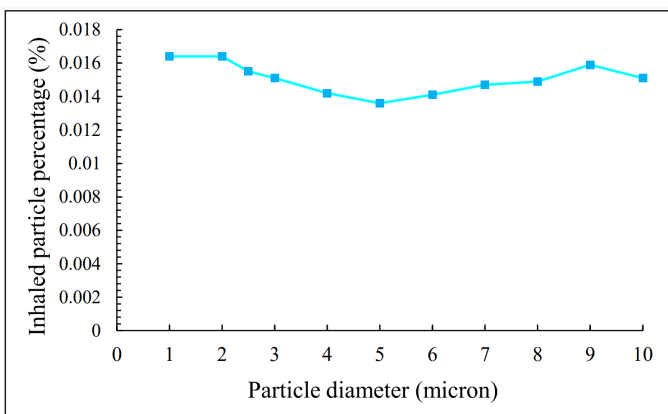


Figure 13: Inhaled particle percentage.



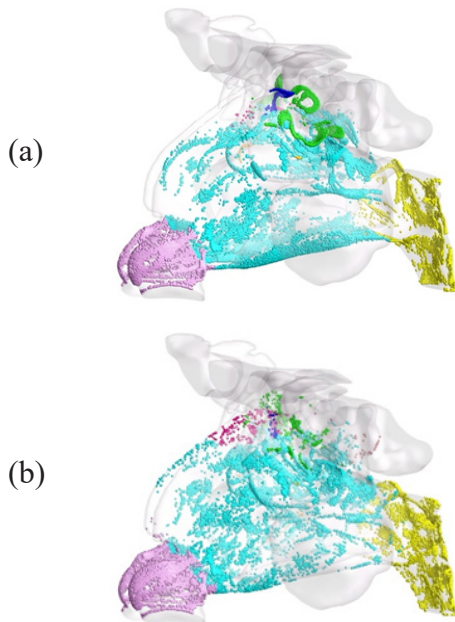


Figure 16: Deposited particles on the nasal cavity: (a) 1 micron; (b) 10 micron.

has been decreased and almost no particles have been reached to the ceiling wall. The same analysis can be extended to the aspiration fractions as demonstrated in **Figure 12**. For more reliable results, the 20- $\mu\text{m}$  particles were analyzed in this figure.

## Conclusion

Although the wind catchers have capability to reduce the energy consumption as a result of natural ventilation, they may be harmful for the respiratory system based on where they are used and the concentration of micro particles.

The present study is aimed to enlighten the portion of particles inhaled by a nasal route. Based on the obtained results and according to the number of particles delivered to the outlet of the nasal cavity, the most detrimental particles to the respiratory system in the order are: 1, 2, 2.5, 3, 4, 7, 9, 6, 8, 5, and 10. This order according to the mass of particles delivered is: 10, 9, 8, 7, 6, 5, 4, 3, 2.5, 2, and 1. The findings in the present study are analogous to results presented in the literature that *PM10* particulate matters are the most perilous for the human respiratory system; Because after 10 micron the aspiration fraction of 20-micron particles has dramatically declined; So, the results can be used by specialists to do implications in terms of wind catchers if it is necessary.

**Recommendations for future works:** It is recommended to be employed other scenarios for different inhalation flow rates and the position and direction of the mannequin. The present study has neglected the effect of fluctuating velocity due to the turbulent flow; So, it is better to use CRW instead of DRW. Declaration of competing interest: The authors declare that no conflict of interest exists.

**Acknowledgment:** This research did not receive any specific grant from funding agencies in the public, commercial, or not-for-profit sectors.

## References

1. Shaeri J, Mahdavinejad M, Vakilinejad R, Bazazzadeh H, Monfared M. Effects of sea-breeze natural ventilation on thermal comfort in low-rise buildings with diverse atrium roof shapes in bwh regions. *Case Studies in Thermal Engineering*, 2023; 41. doi: 10.1016/j.csite.2022.102638.
2. Peeters S, Wang C, Bijnens EM, Bullens DM, Fokkens

- WJ, Bachert C, et al. Association between outdoor air pollution and chronic rhinosinusitis patient reported outcomes. *Environmental Health: A Global Access Science Source*, 2022; 21: 1–10. <https://doi.org/10.1186/s12940-022-00948-7>; doi:10.1186/s12940-022-00948-7.
3. Zare F, Aalaei E, Zare F, Faramarzi M, Kamali R. Targeted drug delivery to the inferior meatus cavity of the nasal airway using a nasal spray device with angled tip. *Computer Methods and Programs in Biomedicine*, 2022; 221. doi: 10.1016/j.cmpb.2022.106864.
4. Hayati H, Feng Y, Chen X, Kolewe E, Fromen C. Prediction of transport, deposition, and resultant immune response of nasal spray vaccine droplets using a cfpd—hcd model in a 6-year-old upper airway geometry to potentially prevent covid-19. *Experimental and Computational Multiphase Flow*, 2023. doi: 10.1007/s42757-022-0145-7.
5. Seifelnasr A, Zare F, Si XA, Xi J. Optimized gravity-driven intranasal drop administration delivers significant doses to the ostiomeatal complex and maxillary sinus. *Drug Delivery and Translational Research*, 2023. <https://doi.org/10.1007/s13346-023-01488-4>; doi: 10.1007/s13346-023-01488-4.
6. Tang CX, Dong Y, Yuan XY, Wang R, Wu CC, Bao LJ, et al. Effects of organic carbon/elemental carbon and particle size on inhalation bioaccessibility of particle-bound pahs. *Science of the Total Environment*, 2023; 889. doi: 10.1016/j.scitotenv.2023.164225.
7. Zhu C, Xue Y, Li Y, Yao Z, Li Y. Assessment of particulate matter inhalation during the trip process with the considerations of exercise load. *Science of the Total Environment*, 2023; 866. doi: 10.1016/j.scitotenv.2022.161277.
8. Shi F, Ju J, Zhang X, Zheng R, Xiong F, Liu J. Evaluating the inhalation bioaccessibility of traffic-impacted particulate matter-bound pahs in a road tunnel by simulated lung fluids. *Science of the Total Environment*, 2022; 832. doi: 10.1016/j.scitotenv.2022.155046.
9. Azhdari M, Tavakol MM, Ahmadi G. Particle inhalability of a standing mannequin with large airways in a ventilated room. *Computers in Biology and Medicine*, 2021; 138. doi: 10.1016/j.combiomed.2021.104858.
10. Shang Y, Inthavong K. Numerical assessment of ambient inhaled micron particle deposition in a human nasal cavity. *Experimental and Computational Multiphase Flow*, 2019; 1. doi: 10.1007/s42757-019-0015-0.
11. Montazeri H, Montazeri F. Cfd simulation of cross-ventilation in buildings using rooftop wind-catchers: Impact of outlet openings. *Renewable Energy*, 2018; 118. doi: 10.1016/j.renene.2017.11.032.
12. Vardoulakis S, Giagloglou E, Steinle S, Davis A, Sleenwenhoek A, Galea KS, et al. Indoor exposure to selected air pollutants in the home environment: A systematic review, 2020. doi: 10.3390/ijerph17238972.
13. Kim KH, Kabir E, Kabir S. A review on the human health impact of airborne particulate matter, 2015. doi: 10.1016/j.envint.2014.10.005.
14. Richards PJ, Norris SE. Appropriate boundary conditions for computational wind engineering models revisited. *Journal of Wind Engineering and Industrial Aerodynamics*, 2011; 99. doi: 10.1016/j.jweia.2010.12.008.
15. Blocken B, Stathopoulos T, Carmeliet J. Cfd simulation of the atmospheric boundary layer: wall function problems. *Atmospheric Environment*, 2007; 41. doi: 10.1016/j.atmosenv.2006.08.019.
16. Kelly JT, Asgharian B, Kimbell JS, Wong BA. Particle deposition in human nasal airway replicas manufactured by different methods. part i: Inertial regime particles. *Aerosol Science and Technology*, 2004; 38. doi: 10.1080/027868290883360.
17. Schroeter JD, Garcia GJ, Kimbell JS. Effects of surface smoothness on inertial particle deposition in human nasal models. *Journal of Aerosol Science*, 2011; 42. doi: 10.1016/j.jaerosci.2010.11.002.
18. Rahman M, Zhao M, Islam MS, Dong K, Saha SC. Numerical study of nano and micro pollutant particle transport and deposition in realistic human lung airways. *Powder Technology*, 2022; 402. doi: 10.1016/j.powtec.2022.117364.